ISSN 2616-5775 Vol. 8, Issue 9: 46-53, DOI: 10.25236/AJCIS.2025.080907

DAU-Net: Density-Aware U-Shaped Network for Non-Uniform Haze Removal

Qiang Qu[1], Yingbo Wang[1,*]

[1]*School of Electronic Information and Artificial Intelligence, Shaanxi University of Science and Technology, Xi'an, China, 710021*
[*]*Corresponding author: wangyb_0309@163.com*

Abstract: *Haze in the atmosphere significantly degrades the quality of images captured by sensors by obscuring key visual features, thereby impairing the performance of downstream computer vision tasks. In real-word scenarios, haze often exhibits complex multi-scale characteristics and spatial non-uniformity, posing significant challenges for image dehazing due to severe detail loss and contrast reduction in heavily hazy regions. To address these issues, this paper proposes a novel dehazing method tailored for non-uniform haze removal, based on a haze density-aware U-shaped network architecture. The proposed framework comprises two core components: a haze density perception module and a U-shaped encoder-decoder network built upon NMF (Nonlinear Activation Mamba Fog) blocks. The haze density perception module employs a lightweight convolutional neural network (CNN) to estimate pixel-level haze density maps and adaptively adjusts input weights based on haze density to accommodate scenes with varying haze intensities, thereby effectively enhancing the ability of network's contextual perception under different haze regions. The NMF block replaces conventional nonlinear activation functions with a learnable gating mechanism, facilitating implicit nonlinear transformation while mitigating gradient saturation during training. Moreover, the NMF module adopts a dual-branch structure that integrates: (1) a spatial-channel attention (SCA) mechanism to emphasize informative feature across both spatial and channel dimensions, and (2) a Mamba-based state-space model for range spatial dependency modeling, which captures the global distribution patterns of haze more effectively than local convolutions. Experimental results demonstrate that the proposed method achieves highly competitive performance on non-uniform haze image datasets, effectively improving detail restoration and color fidelity in image dehazing.*

Keywords: *Image Dehazing, Fog Density Estimation, Non-Uniform Haze, Mamba*

1. Introduction

Image dehazing, as a core research direction in low-level vision tasks, focuses on recovering clear and high-contrast haze-free scenes from degraded observed images affected by atmospheric scattering effects. This technology has been widely applied in various fields such as autonomous driving, video surveillance, and remote sensing observation. The degradation of image quality under haze interference not only significantly reduces human subjective visual experience but also severely limits the accuracy and robustness of downstream high-level vision tasks (e.g., object detection and semantic segmentation). In recent years, with the rapid development of deep learning techniques, data-driven image dehazing methods have achieved significant breakthroughs. However, image clarification still faces serious technical challenges under non-uniform haze conditions. In real-world complex atmospheric environments, influenced by factors such as varying scene depths, differences in illumination conditions, uneven spatial distribution of aerosols, and localized pollution sources, haze distribution in images often exhibits distinct spatial non-uniformity [1]. Therefore, designing effective image dehazing methods to recover scene content with clear details and natural visual effects has become a highly valuable research direction in the fields of computer vision and image processing.

Traditional physics-based image dehazing methods, such as the Dark Channel Prior (DCP) and Color Attenuation Prior (CAP), generally demonstrate strong performance under homogeneous haze conditions [2]. However, the statistical priors relied upon by these methods struggle to effectively adapt to the spatial variability of non-uniform haze. This is particularly evident in sky regions, bright objects, or areas with complex textures, where dehazing results often deteriorate. With the rise of deep learning, Convolutional Neural Networks (CNNs) have shown significant performance improvements in image dehazing tasks by automatically learning image features through multi-layer convolution and pooling operations[3]. Despite this, CNN-based methods still exhibit inherent limitations when handling non-uniform haze. Their relatively limited receptive fields make it difficult to effectively capture global contextual information in images, thereby failing to adequately model the distribution patterns of haze and long-range dependencies among objects in a scene.To overcome these limitations, the Transformer architecture has demonstrated unique advantages in feature extraction due to its self-attention mechanism. The self-attention mechanism enables parallel computation of dependencies between all positions in a sequence, breaking the constraints of locality and allowing the model to perform image modeling and analysis from a global perspective [4]. However, the computational complexity of the self-attention mechanism in Transformers grows quadratically with image size, posing a substantial challenge for its application in high-resolution image processing [5].

To address the aforementioned challenges, this paper proposes a novel non-uniform image dehazing network called DAU-Net (Density-Aware U-Net). Its core architecture consists of a haze density perception module and a Nonlinear Activation-Free Mamba Block (NMFBlock), adopting a U-shaped encoder-decoder structure to achieve multi-scale contextual information fusion.Specifically, the method first employs a lightweight convolutional subnetwork to perform pixel-level haze density estimation on the input hazy image, generating a corresponding attention weight map. This weight map is then deeply integrated with the original input features to dynamically adjust the network's focus on regions with varying haze densities, thereby enhancing the model's adaptability to non-uniform haze distribution. Furthermore, this study discards activation functions (such as ReLU) commonly used in traditional networks that may cause gradient saturation issues. Instead, a gating mechanism-based nonlinear mapping function is adopted to improve gradient flow and training stability.The network design incorporates a dual-branch processing mechanism: One branch is the Channel Attention Branch (SCA Branch), which adaptively recalibrates feature channel responses through a channel attention mechanism to highlight informative feature maps. The other branch is the Mamba Branch, which leverages the long-sequence modeling capability of state space models to effectively capture the global spatial context and structural dependencies of haze distribution in the image. By fusing the outputs of these two branches, the model can synergistically enhance local detail features and global semantic representations. Experimental results demonstrate that the proposed DAU-Net achieves significant advantages in both subjective visual quality assessment and objective evaluation metrics, validating its effectiveness and advancement in non-uniform image dehazing tasks.

The contributions of this work can be summarized as follows:

(1) A lightweight haze density perception module is proposed, which employs a compact convolutional subnetwork to estimate pixel-level haze density perception maps. These maps are used to dynamically modulate feature representations according to local haze concentrations, thereby enabling spatially adaptive processing and improving the model's sensitivity to non-uniform atmospheric degradation.

(2) A dual-branch feature enhancement module is designed, integrating a spatial-channel attention (sca) branch and a mamba-based long-range modeling branch. The design leverages implicit nonlinear transformations through a gating mechanism, enhancing feature expressiveness while effectively capturing both channel-wise saliency and global spatial dependencies in hazy scenes.

(3) A haze density-aware u-shaped encoder-decoder architecture is developes, where multi-scale haze density features are progressively extracted in the encoder and fused with high-resolution details via skip connections in the decoder. This hierarchical fusion strategy enables density-guided feature refinement, leading to more accurate and spatially coherent dehazing results under heterogeneous haze conditions.

2. Related Work

2.1 Image Dehazing

Image dehazing serves as a pivotal research direction in low-level vision restoration tasks, aiming to recover clear, high-contrast, and color-fidelity haze-free scenes from degraded observed images affected by atmospheric scattering effects. Traditional image dehazing methods are typically based on the classical atmospheric scattering model, which is mathematically expressed as:

$$I(x) = J(x) \cdot t(x) + A(1 - t(x)) \tag{1}$$

Where $I(x)$ represents the observed haze image, $J(x)$ denotes the haze-free image to be restored, A

ISSN 2616-5775 Vol. 8, Issue 9: 46-53, DOI: 10.25236/AJCIS.2025.080907

stands for the global atmospheric light value, and $t(x)$ is the transmission map of the medium. Early research primarily relied on handcrafted statistical priors to impose regularization constraints on transmission estimation. Among these, the most representative is the dark channel prior proposed by He *et al*. [6]. which, based on statistical analysis of numerous haze-free images, posits that in local regions of an image, at least one-color channel has pixel values approaching zero. Although this prior performs well under conditions of uniform thin haze, it is prone to failure in areas with bright objects (such as white vehicles, clouds, or glass) or sky regions, often leading to noticeable color distortion and halo artifacts.

To address the challenges posed by non-uniform haze, berman *et al*. Proposed a non-local dehazing method [7], which decomposes the image into multiple "haze lines" through clustering operations in color space, thereby modeling the spatial variation characteristics of haze to some extent. However, this method relies on K-means clustering, making it not only sensitive to noise but also introducing high computational complexity. Overall, although physics-based methods can achieve satisfactory results under specific conditions, they struggle to fully adapt to the complex and variable haze distributions in real-world scenarios, particularly exhibiting instability in handling non-uniform dense fog, dynamic weather conditions, or mixed indoor-outdoor environments.

In recent years, with the rapid advancement of deep learning technologies, data-driven image dehazing methods have gradually become the mainstream research direction in this field. The DehazeNet proposed by Cai *et al*. [2]. was the first to utilize a convolutional neural network to directly estimate the transmission map and further combined it with the atmospheric scattering model to restore haze-free images. This method significantly improved the accuracy of transmission estimation through multi-scale feature extraction and fusion strategies. The DCPDN network developed by Zhang and Patel integrated generative adversarial networks (GANs) with physical prior models, leveraging a dual-branch structure to separately estimate transmission and atmospheric light components [8]. The FFA-Net proposed by Qin *et al*. introduced a feature attention mechanism, enhancing the expressive capability of critical features through channel attention and pixel attention modules [9]. The GridDehazeNet designed by Dong *et al*. [10]. employs a grid-like densely connected structure to facilitate feature flow and fusion, though its limited receptive field somewhat constrains its ability to model long-range dependencies. The DehazeFormer proposed by Song *et al*. [11]. adapts normalization methods and activation functions to meet the requirements of image dehazing tasks, demonstrating excellent capability in modeling global dependencies within images, particularly outperforming traditional convolutional methods in complex scenes. The Uformer developed by Wang *et al*. [12]. combines a locally enhanced window mechanism with a learnable multi-scale restoration modulator, utilizing a hierarchical architecture to simultaneously capture local details and global contextual information, achieving outstanding dehazing results while maintaining high computational efficiency.

2.2 Mamba

Mamba is a novel architecture based on the State Space Model (SSM), proposed by Gu and Dao *et al*. in 2023 [13]. Its core innovation lies in introducing an input-dependent selective mechanism, which extends the fixed system parameters of traditional state space models into variables that can be dynamically adjusted based on input, thereby significantly enhancing the modeling capability for complex data distributions. Compared to the widely used Transformer architecture, Mamba demonstrates multiple advantages in image dehazing tasks [14]. First, Mamba has linear computational complexity $O(L)$, which is significantly lower than the quadratic complexity $O(L^2)$ caused by the self-attention mechanism in Transformers. This characteristic makes it more scalable and computationally efficient when processing high-resolution images. Second, haze in images often exhibits significant spatial inhomogeneity, with considerable variations in concentration and depth across different regions. The selective mechanism of the Mamba model enables it to adaptively focus on thick and thin haze areas based on the input image content, achieving spatial awareness and differentiated processing of varying haze concentrations. This capability not only helps more accurately remove haze interference but also better preserves image details and structural consistency during the restoration process [15].

In summary, with its linear complexity and input-dependent selective state mechanism, Mamba offers a new approach for image dehazing tasks that balances efficiency and performance, particularly suitable for haze scenarios with complex spatial distributions.

3. Method

This section elaborates on the proposed non-uniform image dehazing network (DAU-Net) based on

ISSN 2616-5775 Vol. 8, Issue 9: 46-53, DOI: 10.25236/AJCIS.2025.080907

haze density perception and the Nonlinear Activation Mamba Module (NMFBlock). As illustrated in Fig. 1, the network adopts an encoder-decoder architecture. The first stage employs an extremely lightweight sub-network to estimate a pixel-level haze density map. The second stage utilizes this density map as prior information to accomplish the task of clear image reconstruction within an improved U-shaped encoder-decoder framework. The following sections will discuss these two core modules in detail. Use 18-point font for the title of article, aligned to the left and font bold, with single line space and all the initial letters capitalized. No formulas or special characters of any form or language are allowed in the title.

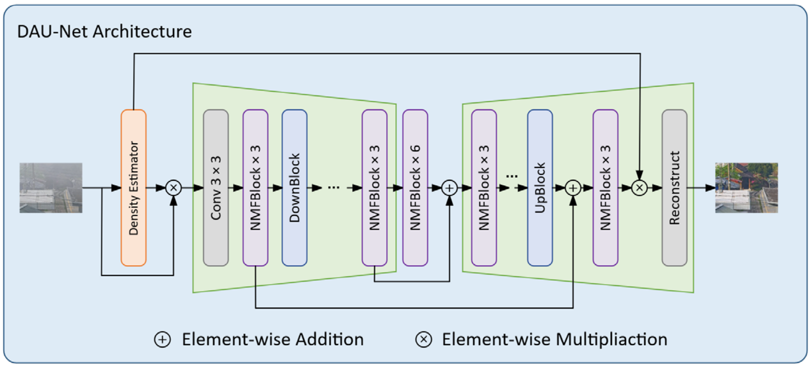

Figure 1: Overall Architecture Diagram of DUA-Net.

3.1 Extraction of Pixel-Level Confidence

The core challenge of non-uniform haze lies in its spatial heterogeneity, where haze concentration varies significantly across different regions of an image. To address this challenge, this paper designs a lightweight haze density estimator aimed at directly regressing a pixel-level haze density map D from the hazy input image $I_{hazy.}$ As shown in Figure 1, this estimator consists of a 3×3 convolutional layer, a ReLU activation function, and a 1×1 convolutional layer connected sequentially. The computational process can be expressed mathematically as follows:

$$D = \varepsilon(I_{hazy}) = \sigma(C_{1\times1}(\phi(C_{3\times3}(I_{hazy})))) \tag{2}$$

Where $C_{3\times3}$ and $C_{1\times1}$ denote convolutional operations with kernel sizes of 3×3 and 1×1, respectively. ϕ represents the ReLU activation function, and σ represents the Sigmoid activation function, which is used to normalize the output density values to the range [0,1]. A density value closer to 1 indicates a higher haze concentration in the corresponding region. This density map D will be further utilized to generate an adaptive weight map and fused with the original input image through element-wise multiplication to obtain the weighted input image $I_{weighted}$:

$$I_{weighted} = I_{hazy} \odot (1 + \alpha \cdot D) \tag{3}$$

Where $\odot$ denotes element-wise multiplication, and α is a learnable scaling factor. This mechanism enables the network to focus its attention on regions with higher haze concentrations, facilitating differentiated processing of heavily hazed areas. Consequently, it provides spatially adaptive guidance for the subsequent image restoration backbone network.

3.2 NMFBlock-based Encoder-Decoder Restoration Network

As illustrated in Figure 1, the proposed network adopts a three-level encoder-decoder architecture. At each level of the encoder, three NMF Blocks are first connected in series for multi-scale feature extraction, followed by a 2×2 convolutional layer with a stride of 2 to perform downsampling while doubling the number of channels. In the bottleneck layer, a total of six NMF Blocks are stacked to capture high-level semantic information of the image. The decoder employs Pixel-Shuffle operations for upsampling, simultaneously halving the number of channels, and incorporates skip connections to fuse features from the corresponding encoder level, thereby compensating for potential detail loss during downsampling. Both the input and output ends of the network utilize 3×3 convolutions to map between the image and feature domains. Finally, a global residual connection is applied to reconstruct the clear image.

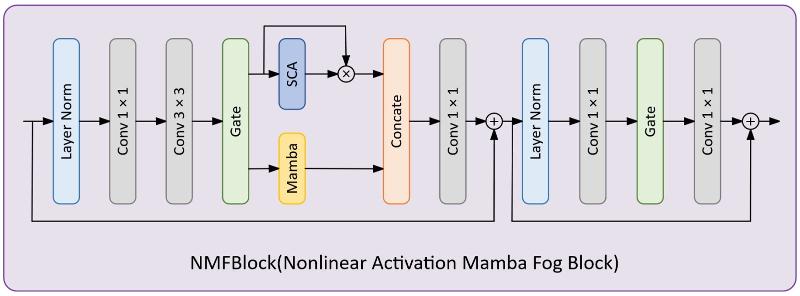

Figure 2: Nonlinear Activation Mamba Fog Block Structure Diagram.

The NMFBlock (Nonlinear Activation Mamba Fog Block), serving as the core feature extraction unit of the network, is detailed in Figure 2. This module employs a gating mechanism to achieve efficient nonlinear transformation and simultaneously models channel attention and long-range spatial dependencies through a dual-branch structure. For an input feature X, Layer Normalization is first applied to standardize the input, enhancing training stability. Subsequently, a 1×1 pointwise convolution expands the channel dimension to twice the original size (i.e., 2C), followed by a 3×3 depthwise separable convolution to further extract local spatial features. The resulting features are then split evenly along the channel dimension into two parts, X_1 and X_2, and a gating mechanism is implemented via element-wise multiplication to ultimately generate the nonlinear output:

$$Gate(X) = X_1 \odot X_2 \tag{4}$$

Subsequently, the gated features are fed into two parallel branches. The channel attention branch first aggregates global channel information through global average pooling and employs a multilayer perceptron to generate channel weights, thereby recalibrating the original features to enhance the response intensity of critical channels. The other branch is the Mamba branch, which incorporates a State Space Model (SSM). Leveraging its linear complexity and powerful long-range sequence modeling capabilities, this branch effectively captures global spatial contextual information within the image. The outputs of the two branches are concatenated along the channel dimension and then passed through a 1×1 convolutional layer for feature fusion and dimensionality reduction. The result is integrated with the original input via a residual connection. Finally, the module further enhances its nonlinear representational capacity through channel adjustment and a gated residual mechanism.

4. Experiments

To comprehensively evaluate the performance of the proposed haze density perception and NMFBlock-based non-uniform image dehazing network (DAU-Net), this chapter conducts systematic experiments on public datasets. The evaluation is carried out from three main dimensions: experimental setup, result analysis, and validation on advanced vision tasks, with a particular focus on analyzing DAU-Net's advantages in detail preservation and color fidelity.

4.1 Experimental Settings

This experiment was conducted on the widely adopted benchmark non-uniform hazy image dataset RW2AH for both training and testing. The training set consists of 800 images with a resolution of 640×540, while the test set contains 100 images. To comprehensively evaluate the performance of the proposed method, three representative state-of-the-art image dehazing algorithms were selected as comparative approaches. All methods were trained on the same training set using a consistent strategy until model convergence and were evaluated quantitatively and qualitatively on the same test set.

This model was implemented based on the PyTorch 2.4 deep learning framework and the Accelerate distributed training library, supporting mixed-precision computation and multi-GPU parallel training. The hardware platform utilized an Nvidia rtx 3090 GPU. The AdamW optimizer was employed with parameters configured as β_1=0.9 and β_2=0.999. The initial learning rate was set to 5e-5 and adaptively adjusted using a Cosine Annealing Schedule. The training batch size was 20, with a total of 150k iterations. The loss function adopted a dynamically weighted combination of L1 and Mean Squared Error (MSE): during the initial training phase, MSE dominated (weight coefficient 0.9), transitioning to L1 dominance (final weight 1.0) through a piecewise linear decay strategy. A gradient clipping threshold of 5.0 was applied to effectively suppress gradient anomalies in dense haze regions.

ISSN 2616-5775 Vol. 8, Issue 9: 46-53, DOI: 10.25236/AJCIS.2025.080907

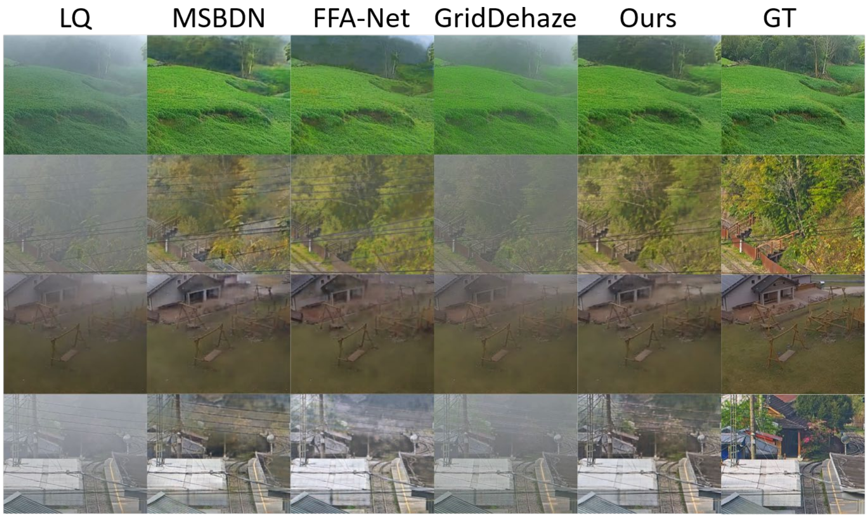

Figure 3: The qualitative results of this method compared with other methods on the RW2AH test set.

4.2 Comparison of experimental results with other methods

Figure 3 presents qualitative comparison results on the test set. The first row of samples depicts a typical scenario where haze concentration increases progressively from the foreground to the background. Compared with other comparative methods, the haze density map generated by DAU-Net accurately identifies the haze concentration distribution across different regions while demonstrating superior color restoration. Vegetation areas exhibit more realistic emerald green tones, with natural color transitions and significantly enhanced spatial depth perception. The fourth row of samples contains noticeably non-uniform haze distribution in the background regions. Existing comparative methods show limited restoration effectiveness in this scenario, manifesting as loss of road texture and halo artifacts at haze boundaries. Leveraging the local-global joint modeling mechanism of its NMFBlock module, DAU-Net effectively captures the spatial continuity and long-range dependencies of haze. It achieves smooth transitions under complex distributions where thin haze in the foreground coexists with thick haze in the distance, producing highly consistent restoration results overall and demonstrating exceptional detail preservation capabilities, particularly in texture-rich regions.

Figure 4 presents a comparison of the average PSNR and SSIM performance of various methods on the test set. Experimental results demonstrate that the proposed method achieves a PSNR value of 21.785 dB, significantly outperforming all comparative approaches and improving by 0.482 dB over the second-best model, MSBDN. This highlights DAU-Net's superiority in pixel-level reconstruction accuracy and detail recovery. In terms of structural similarity, the proposed method also achieves the highest SSIM score of 0.574, further validating the structural consistency of its restoration results. Based on comprehensive qualitative and quantitative evaluations, DAU-Net not only exhibits higher restoration accuracy and visual naturalness in non-uniform haze distribution scenarios but also maintains strong computational efficiency, fully demonstrating the effectiveness and advancement of the proposed haze density perception mechanism and the synergistic design of NMFBlock.

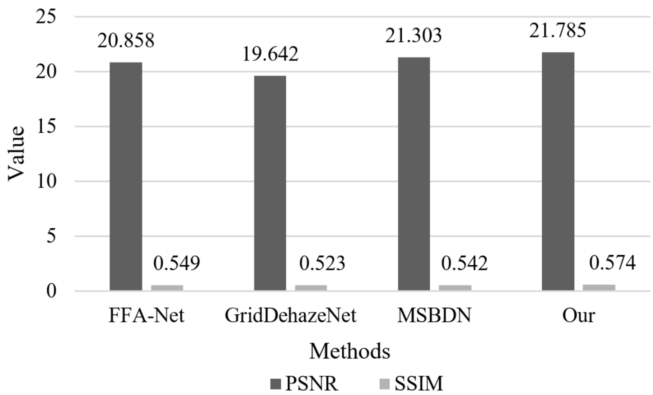

Figure 4: Statistical analysis quantitative indicators.

4.3 More Experiments and Analyses

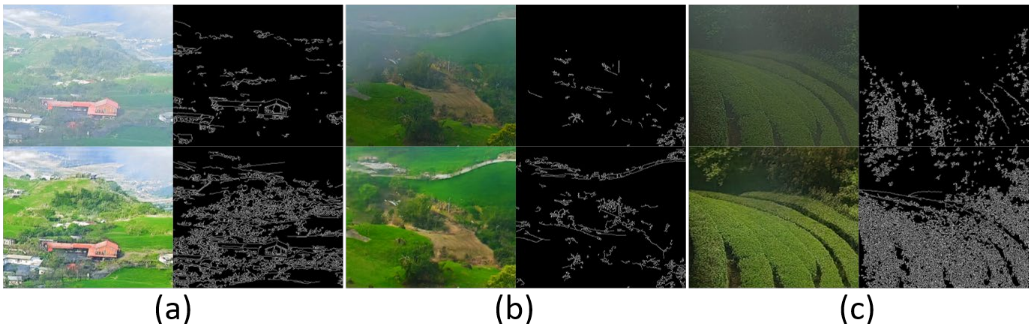

Figure 5: The edge detection results of the Canny edge detection algorithm on foggy images (top) and restored images (bottom).

To evaluate the promoting effect of DAU-Net's image dehazing results on high-level vision tasks, this study employs edge detection as a representative downstream task to comparatively analyze the differences in structural preservation and detail discernibility before and after dehazing. The experiment utilizes the Canny edge detection operator under consistent parameter settings to process images from the test set. As shown in Figure 5, other methods exhibit generally weaker edge responses due to overall contrast attenuation in hazy images, with particularly noticeable breaks in distant regions. Additionally, noise interference caused by non-uniform haze distribution leads to false edge responses in some smooth areas (e.g., the sky). In contrast, images restored by DAU-Net show significantly improved edge continuity, with effective recovery of high-frequency information such as distant building contours and branch details. This indicates that the network effectively preserves structural integrity at object boundaries while removing non-uniform haze. In summary, DAU-Net successfully reconstructs high-frequency structural features in images, enhancing edge localization accuracy while suppressing false edges. This provides a more reliable structural information foundation for high-level vision tasks such as object detection, semantic segmentation, and stereo matching.

5. Conclusions

To address the challenge that traditional dehazing methods struggle to balance global consistency and local detail restoration in non-uniform haze distribution scenarios, this paper proposes an image dehazing network called DAU-Net, which is based on haze concentration awareness and a Nonlinear activation Mamba module (NMFBlock). By integrating haze-aware priors with a content-adaptive restoration mechanism, this proposed method achieves superior dehazing performance and visual fidelity while maintaining a lightweight model architecture. The designed lightweight haze concentration estimation subnetwork generates pixel-level haze concentration estimation maps without relying on ground-truth transmission maps, enabling effectively guiding the subsequent network to enhance features in high-haze regions and alleviating the insufficient restoration of dense haze areas in traditional methods. Furthermore, this paper introduces the Nonlinear activation Mamba module (NMFBlock), a hybrid feature extraction module that combines local convolutional processing with state-space modeling. This integration enables efficient long-range spatial dependency modeling at linear computational complexity, significantly enhancing the network's capacity to adapt to spatially varying haze distributions. Experimental results demonstrate that DAU-Net achieves remarkable performance in both quantitative and qualitative evaluations, particularly exhibiting superior robustness and detail restoration capabilities in non-uniform haze scenarios. In summary, by effectively integrating physical priors and deep learning mechanisms, DAU-Net provides an efficient, robust, and scalable solution for non-uniform image dehazing tasks, offering new insights and references for related research.

References

[1] Ancuti C O, Ancuti C, Timofte R. NH-HAZE: An image dehazing benchmark with non-homogeneous hazy and haze-free images[C]//Proceedings of the IEEE/CVF conference on computer vision and pattern recognition workshops. 2020: 444-445.

[2] Cai B, Xu X, Jia K, et al. Dehazenet: An end-to-end system for single image haze removal[J]. IEEE transactions on image processing, 2016, 25(11): 5187-5198.

ISSN 2616-5775 Vol. 8, Issue 9: 46-53, DOI: 10.25236/AJCIS.2025.080907

[3] Ren W, Ma L, Zhang J, et al. Gated fusion network for single image dehazing[C]//Proceedings of the IEEE conference on computer vision and pattern recognition. 2018: 3253-3261.
[4] Chen H, Wang Y, Guo T, et al. Pre-trained image processing transformer[C]//Proceedings of the IEEE/CVF conference on computer vision and pattern recognition. 2021: 12299-12310.
[5] Sakaridis C, Dai D, Van Gool L. ACDC: The adverse conditions dataset with correspondences for semantic driving scene understanding[C]//Proceedings of the IEEE/CVF international conference on computer vision. 2021: 10765-10775.
[6] He K, Sun J, Tang X. Single image haze removal using dark channel prior[J]. IEEE transactions on pattern analysis and machine intelligence, 2010, 33(12): 2341-2353.
[7] Berman D, Avidan S. Non-local image dehazing[C]//Proceedings of the IEEE conference on computer vision and pattern recognition. 2016: 1674-1682.
[8] Zhang H, Patel V M. Densely connected pyramid dehazing network[C]//Proceedings of the IEEE conference on computer vision and pattern recognition. 2018: 3194-3203.
[9] Qin X, Wang Z, Bai Y, et al. FFA-Net: Feature fusion attention network for single image dehazing[C]//Proceedings of the AAAI conference on artificial intelligence. 2020, 34(07): 11908-11915.
[10] Liu X, Ma Y, Shi Z, et al. Griddehazenet: Attention-based multi-scale network for image dehazing[C] //Proceedings of the IEEE/CVF international conference on computer vision. 2019: 7314-7323.
[11] Song Y, He Z, Qian H, et al. Vision transformers for single image dehazing[J]. IEEE Transactions on Image Processing, 2023, 32: 1927-1941.
[12] Wang Z, Cun X, Bao J, et al. Uformer: A general u-shaped transformer for image restoration[C] //Proceedings of the IEEE/CVF conference on computer vision and pattern recognition. 2022: 17683-17693.
[13] Gu A, Dao T. Mamba: Linear-time sequence modeling with selective state spaces[J]. arXiv preprint arXiv:2312.00752, 2023.
[14] Zou Z, Yu H, Huang J, et al. Freqmamba: Viewing mamba from a frequency perspective for image deraining[C]//Proceedings of the 32nd ACM international conference on multimedia. 2024: 1905-1914.
[15] Guo H, Li J, Dai T, et al. Mambair: A simple baseline for image restoration with state-space model[C]//European conference on computer vision. Cham: Springer Nature Switzerland, 2024: 222-241.